



Calhoun: The NPS Institutional Archive
DSpace Repository

Faculty and Researchers

Faculty and Researchers' Publications

2018-03

Application of equivalent medium parameters in finite element models of microwave metamaterials

Hewitt, C.; Alves, F.; Luscombe, J.; Grbovic, D.

<https://hdl.handle.net/10945/57875>

This publication is a work of the U.S. Government as defined in Title 17, United States Code, Section 101. Copyright protection is not available for this work in the United States.

Downloaded from NPS Archive: Calhoun



Calhoun is the Naval Postgraduate School's public access digital repository for research materials and institutional publications created by the NPS community. Calhoun is named for Professor of Mathematics Guy K. Calhoun, NPS's first appointed -- and published -- scholarly author.

Dudley Knox Library / Naval Postgraduate School
411 Dyer Road / 1 University Circle
Monterey, California USA 93943

<http://www.nps.edu/library>

Application of equivalent medium parameters in finite element models of microwave metamaterials

C. Hewitt, F. Alves, J. Luscombe, and D. Grbovic^{a)}

Physics Department, Naval Postgraduate School, Monterey, California 94043, USA

(Received 4 October 2017; accepted 1 March 2018; published online 16 March 2018)

Simulated or experimentally measured reflection and transmission are used to obtain effective permittivity (ϵ), permeability (μ), and conductivity (σ) for a planar microwave metamaterial. These parameters are then used in a finite element model of macro-scale metamaterial objects, where the metamaterial is taken to be a homogeneous layer with frequency-dependent ϵ , μ , and σ . We demonstrate good agreement between reflection and absorption of metamaterial structure and those obtained from modeling homogenized, macro-scale metamaterials. We further demonstrate use of the method for geometrically scaled, oddly shaped macroscopic objects. This method significantly reduces computation requirements and enables modeling of metamaterial-made, large area objects without modeling their actual intricate metamaterial structure. <https://doi.org/10.1063/1.5008279>

I. INTRODUCTION

Electromagnetic metamaterials are being developed and employed in a variety of applications such as sensing,¹ imaging and optics,² signature reduction and cloaking,³ and electromagnetic protection.⁴ Metamaterials are typically designed as composite structures consisting of patterned, conductive elements integrated with dielectric materials and arrayed in a manner that generates a desired, predictable spectral response.⁴ Depending on the application, such metamaterials can become structurally complex, which makes them difficult to model, particularly across a large frequency domain. In such cases, a parametrization of the metamaterial based on the concept of an equivalent medium can be useful for easing the computational cost of modeling.⁴⁻⁸

In this paper, we report on a method for retrieving equivalent medium parameters from single- and multi-band planar metamaterial perfect absorbers (shown in Fig. 1), and then using those parameters to streamline modeling and design. This method uses reflection and transmission scattering parameters either from simulation or experimental measurement of metamaterial samples. Reflection coefficient (S_{11}) and transmission coefficient (S_{21}) are used in a system of equations to calculate the frequency-dependent permittivity, permeability, and conductivity of an equivalent homogeneous material. The rationale for the process is that the use of homogenized parameters can radically simplify the modeling of complex structures covered with or made from metamaterials. The results are simplified computer models which closely mimic the performance of the original, structurally complex metamaterial, and can be readily applied to geometrically large structures (relative to the size of metamaterial unit cell).

Numerous methods have been developed that consider electromagnetic metamaterials as homogeneous structures, parameterized with frequency-dependent material properties such as permittivity and permeability, as reviewed in Ref. 5. Such approaches typically rely on inverse trigonometric

functions. Inverse trigonometric functions are difficult to apply because of the ambiguity involved in selecting the appropriate periodic branch of the function.⁵⁻⁷ Resolving branch ambiguity requires prior knowledge of at least some of the parameters we are trying to determine. For example, one method requires that the material index of refraction be known for at least one frequency, which is then used to extrapolate the refractive index in other parts of the spectrum.⁶⁻⁸ Other methods require parameters collected for multiple thicknesses of the material^{5,6} or parameters collected across multiple frequencies,⁶ in order to extrapolate the correct propagation mode. The method used in this article addresses branch ambiguity through the ratio between the equivalent medium transmission path and effective wavelength in the medium.⁸ Although previously proposed methods determine the effective permittivity and permeability for a metamaterial, to model the attenuation within a medium along with the scattering parameters, our finite element (FE) model requires the effective electrical conductivity, not considered in prior methods. Finally, prior research has rarely extrapolated the performance of the retrieved parameters outside the unit cell analyzed.^{6,7} Our method retrieves parameters valid not only for unit cells but also for macroscopic structures.

II. METHOD

In order to model metamaterial as a homogenized medium, the metamaterial unit cells should ideally have a physical size 10–30 times smaller than the reference wavelength being absorbed.⁸ A periodic structure of such small elements would function as a truly homogenized medium with frequency-dependent, equivalent parameters valid for all incident angles. The metamaterials reported in this paper do not meet this homogenization criterion, as the resonator sizes are no more than three times smaller than the incident wavelengths in some portions of the spectrum of interest. For this metamaterial, the homogenized parameters should be considered *equivalent medium parameters*, which provide a good agreement with experimental values for scattering

^{a)} Author to whom correspondence should be addressed: dgrbovic@nps.edu.

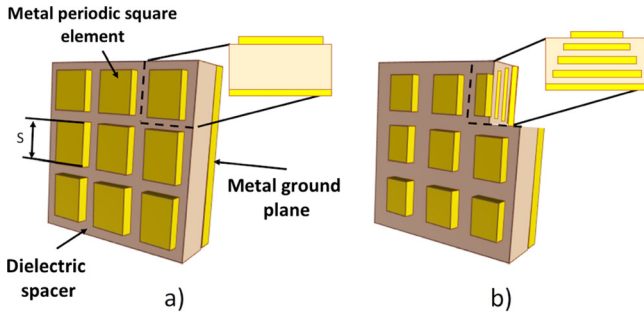


FIG. 1. (a) Cartoon of a typical single-band, planar, metal/dielectric metamaterial perfect absorber where the absorption frequency response is a function of the inverse of the periodic metal square size and the index of refraction of the dielectric spacer; (b) cartoon of a multiband metamaterial with several vertically spaced metallic periodic elements.

and dissipation characteristics within the medium at near-normal angles of incidence. They are rendered ineffective at more extreme incident angles.⁸

We start with the method developed in Ref. 5. To simplify notation, we introduce the *normalized transmission coefficients*⁵

$$t' = te^{ikd}, \quad (1)$$

where $k = \omega/c$ is the wavenumber of the incident radiation and the magnitude of transmission coefficient t is small (in our simulation, on the order of 10^{-4}) for metamaterials with continuous ground plane.

Using reflection coefficient ($r = S_{11}$) and normalized transmission coefficient ($t' = S_{21}e^{ikd}$), we calculate impedance as⁵

$$z = \sqrt{\frac{(1+r)^2 - t'^2}{(1-r)^2 - t'^2}}. \quad (2)$$

In order to extract permittivity and permeability, we require the metamaterial effective index of refraction n which can be obtained by solving⁵

$$\cos(nkd) = \frac{1}{2t'} [1 - (r^2 - t'^2)], \quad (3)$$

where d is the thickness of homogenized metamaterial that will behave optically and electrically in the same manner as the original metamaterial. In this case, we approximated d as equal to twice the metamaterial physical thickness. A problem that arises in applying this equation to metamaterials with a solid ground plane is that transmission is near-zero, as confirmed by both simulation and experiment (ground plane in our case is thicker than the skin depth for the frequencies of interest). In order to use Eq. (3) to derive equivalent medium parameters, it is necessary to use a transmission term that is negligible but non-zero (in our simulation, on the order of 10^{-4}). From the above equation, the complex components of n are solved as positive roots of⁵

$$Im(n) = \pm Im \left(\frac{\cos^{-1} \left(\frac{1}{2t'} [1 - (r^2 - t'^2)] \right)}{kd} \right), \quad (4)$$

$$Re(n) = \pm Re \left(\frac{\cos^{-1} \left(\frac{1}{2t'} [1 - (r^2 - t'^2)] \right)}{kd} \right) + \frac{2\pi m}{kd}, \quad (5)$$

where the integer m refers to the propagation mode through the metamaterial and should be approximately equal to the ratio between the transmission path and the wavelength in the material.⁸ Due to the branch ambiguity arising from the solutions for n (\cos^{-1}), it is crucial that propagation through the metamaterial be described by a single mode.⁸ As noted in Ref. 8, a highly absorbent material with a high index of refraction can result in a medium path length (d) several times longer than the wavelength in the medium (λ/n), despite the small physical thickness of the sample. Therefore, it is necessary to ascertain a consistent propagating mode that meets the criteria $m \approx nd/\lambda$.⁸

Using refractive index n and impedance z , electric permittivity ϵ , magnetic permeability μ , and conductivity σ are obtained using

$$\epsilon = \frac{n}{z} \quad \mu = nz \quad \sigma = \left(\frac{d}{Az} \right), \quad (6)$$

where A is the surface area of the metamaterial unit cell.

Equations (1)–(6) were implemented as a piecewise algorithm operating in the frequency range of interest and used to solve for desired parameters at each frequency. The algorithm is illustrated in Fig. 2. Reflection coefficients were obtained from the scattering parameter S_{11} measurements, imported either from simulated models or from experimental measurements. Transmission on the order of 10^{-4} was assumed across the whole frequency range, given that transmission through the copper ground plane is expected to be negligible. Any remainder, not accounted for by reflection or transmission, was assumed to be resistive attenuation within the metamaterials, as second order scattering can be considered negligible for such structures.⁹

The analysis of the metamaterial structures was performed by finite element (FE) modeling using the radio frequency module of COMSOL multiphysics software. The periodic nature of the metamaterial structures allows the

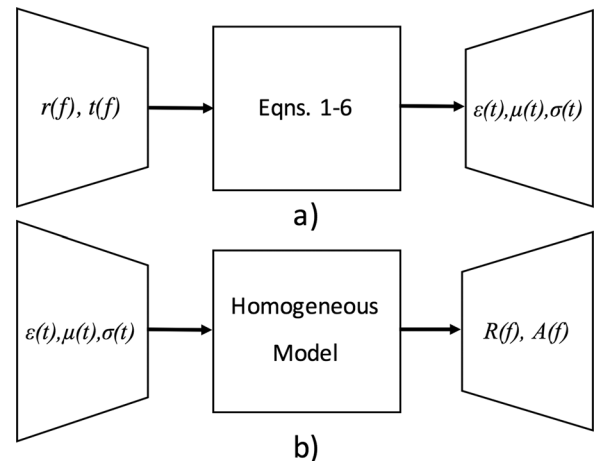


FIG. 2. Schematic diagram of (a) retrieval algorithm and (b) using of the retrieved parameters in the homogeneous model to obtain reflection and absorption.

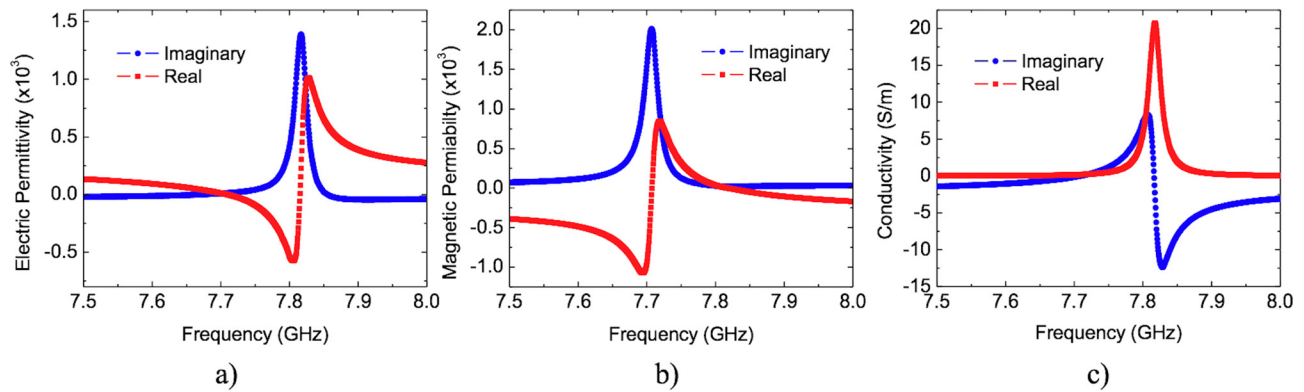


FIG. 3. Retrieved equivalent medium parameters for (a) permittivity, (b) permeability, and (c) conductivity. The peaks in permittivity and conductivity and the well in permeability correspond to the frequency of maximum absorption in the metamaterial spectrum.

simulation to be performed in a unit cell using periodic (Floquet) boundary conditions on the sides and ports on top and bottom of the unit cell. The combination of the active port (1) and the passive port (2) allows retrieval of the scattering parameters in the structure, from which reflection ($R = |S_{11}|^2$) and transmission ($T = |S_{21}|^2$) can be determined. The constituent material properties were measured in the samples using Lucas Signatone 4-point probe (metal) and Filmetrics F-40 (dielectric). A detailed explanation of the modeling procedures can be found in Refs. 2,10, and 11.

III. RESULTS

To verify the concept for the retrieval process, we have applied this method to four cases: (a) simulated reflection data for single-band planar metamaterial, (b) simulated reflection data for multi-band planar metamaterial, (c) experimental reflection data for multi-band planar metamaterial, and (d) simulated reflection data from open literature.

Simulated reflection data were extracted from a simple, single-band, microwave absorbent metamaterial [as shown in Fig. 1(a)], made of copper and FR4, whose square unit cell periodicity is 11 mm, square size is 8.8 mm, and thickness is 146 μm , giving a resonant peak at 7.78 GHz. The retrieval algorithm extracted the equivalent medium parameters from the scattering parameters, and they were then applied to a simulated homogenized medium with depth d . For branch 1, the index of refraction at resonant frequency was found to be 134. When the

equivalent medium depth of 293 μm is multiplied by the index of refraction, the product is 39 mm, the same as the wavelength at resonance. Thus, the criteria⁸ $m \approx nd/\lambda \approx 1$ was satisfied for branch 1. Figure 3 shows the obtained homogenized metamaterial permittivity, permeability, and conductivity, obtained using Eq. (6).

Figure 4(a) shows the simulated reflection used as input to those predicted by two different sizes of homogenized finite element models for branch 1. The two homogenized models are as follows: one with length and width matching the width of the metamaterial unit cell, and another a macroscopic scale model consisting of a flat plate with length and width 20 times greater than the metamaterial unit cell (meant to simulate a notional metamaterial structure). Since the higher order scattering in metamaterial like this can be considered negligible⁹ and there is almost no transmission, it is reasonable to assume that whatever was not reflected was dissipated as heat.¹⁰ The absorption in each model was verified with the volume integration of Joule heating losses, normalized to the model incident power. Figure 4(b) compares the simulated metamaterial resistive losses with the predicted resistive losses from the homogenized model.

The same retrieval procedure was followed with data from a simulated multiband planar metamaterial structure consisting of six resonator layers shown in Fig. 1(b). The multiband square unit cell has a size of 11 mm and thickness of 922 μm . Each unit cell, with a pitch of 11 mm, contains six concentric copper resonator layers varying in width from

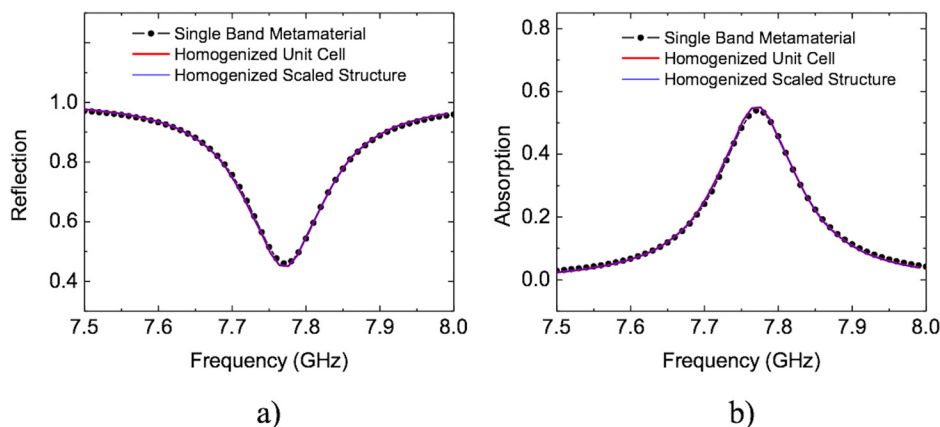


FIG. 4. Comparison of data from single-band unit cell model used as input (blue curve with black markers), 11 mm homogenized unit cell model (red curve), and 22 cm homogenized macroscopic scale model (blue curve) for (a) reflection (b) absorption. Homogenized models used ϵ , μ , and σ obtained using the proposed method. Reflection was derived from the scattering parameters. Absorption was estimated from resistive losses calculated from volume integration of Joule heating normalized to the input power.

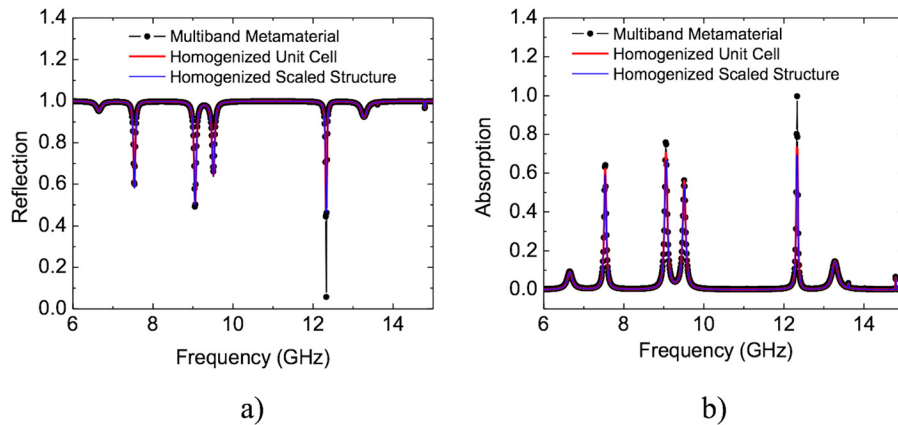


FIG. 5. (a) Comparison of data from multiband unit cell model used as input (blue curve with black dots), 11 mm homogenized unit-cell-sized model (red curve), and 22 cm homogenized macroscopic-size model (green curve) for (a) reflection and (b) absorption. Homogenized models used ϵ , μ , and σ obtained using the proposed method. Reflection was derived from the scattering parameters. Absorption was estimated from resistive losses calculated from volume integration of Joule heating.

5 mm to 10 mm stepped in 1 mm increments. The retrieved parameters were applied to a corresponding homogenized structure. For branch 4, the index of refraction at the resonant frequency, 7.54 GHz, was found to be 87. When the index of refraction was multiplied by the equivalent medium depth 1.844 mm, the product was 160 mm, approximately 4 times the 40 mm wavelength at 7.54 GHz. The outcome of $m \approx nd/\lambda \approx 4$ remained consistent at the resonant points in the spectrum. Figure 5 shows simulation comparisons for reflection and resistive losses between the original simulated data used as input and the output from homogenized structures of two different sizes.

The multi-band metamaterial structure was fabricated by means of a commercial printed circuit board (PCB) foundry using copper resonator layers interspersed with layers of dielectric material (in this case two grades of circuit board fiberglass), anchored on a continuous copper ground plane. Figures 6(a) and 6(b) show the top view of the entire array structure and a single unit cell, respectively. Figure 6(c) shows a Scanning Electron Microscope (SEM) micrograph of a unit cell cross section. SEM measurements were averaged and the horizontal dimensions are in good agreement with the design parameters. The vertical separation between resonators, on the other hand, showed a large variation along the structure, rather different from the design.

Scattering parameters were measured from a plate with a 20×20 array of 11 mm unit cells as shown in Fig. 7, using Agilent N5230A PNA-L network analyzer in monostatic configuration with transmitting/receiving antenna 2 m away from the structure. The retrieval algorithm was used with the experimental scattering data, where branch 4 was also chosen. A comparison of the measurement and homogenized

data can be seen in Fig. 7. Although the models still generate discrepancies at the points of greatest absorption, overall the homogenized predictions show reasonable agreement with the measured input data. We believe that the discrepancies arise from a violation of the homogenization criteria for the propagation mode and that the mode that accurately describes propagation through most of the spectrum does not describe propagation at the points of high attenuation.

In order to verify the retrieval procedure for different material/metamaterial configurations and at different frequency ranges, we have used the scattering parameters for the metasurface epsilon-near-zero (ENZ) based electromagnetic wave absorber studied in Ref. 12. There, an isotropic ENZ material slab is sandwiched by a homogeneous conducting ground plane and a cross shaped metallic element. The dimensions are set on the order to obtain resonant reflection in the near infrared region (150 to 250 THz). Figure 8 shows the reflection of the ENZ metamaterial structure at normal incidence (circular markers) in good agreement with the response obtained using our method (solid line). The scales on the graphs axes are shown in dB and THz for y and x , respectively, to be consistent with the published results in Ref. 12.

IV. USING RETRIEVED PARAMETERS ON ALTERNATE GEOMETRIES

Although the homogenized unit cell and flat plate macroscopic models represent a sound approximation of the actual metamaterials used, the ultimate goal is to be able to change not only the size but also the geometry of the homogenized model and still obtain a good approximation for

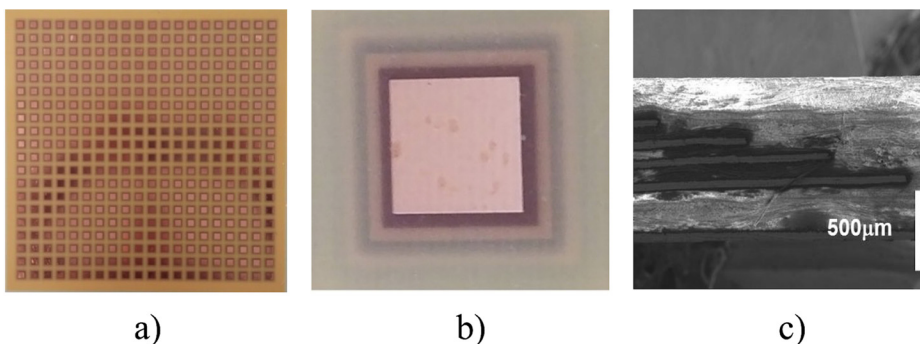


FIG. 6. (a) Photograph of sample metamaterial test plate. (b) Close-up of unit cell and (c) SEM micrograph of the cross section of a metamaterial unit cell.

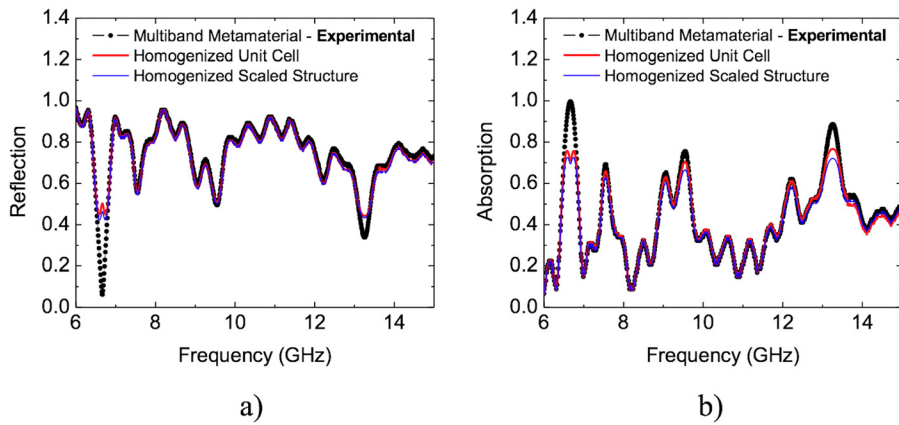


FIG. 7. Comparison of output from multiband sample experimental data model used as input (blue curve with black dots), 11 mm homogenized unit cell model (red curve), and 22 cm homogenized macroscopic scale model (green curve) for (a) reflection and (b) absorption. Reflection was derived from the scattering parameters. Absorption was estimated from resistive losses calculated from volume integration of Joule heating normalized to the input power.

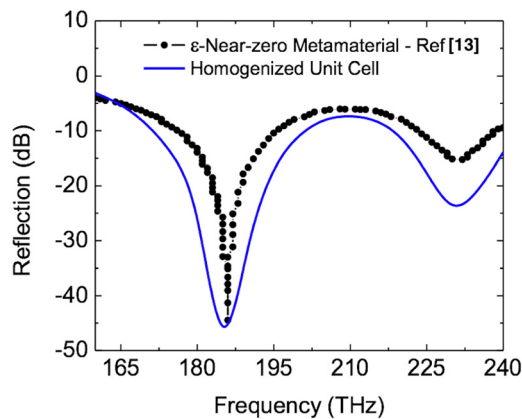


FIG. 8. S_{11} parameter of the metasurface ENZ-based electromagnetic wave absorber studied in Ref. 12 (circular markers), compared with the response obtained using the method described in this paper (solid line).

overall performance. Figure 9(a) shows simulation results of a 1 meter long metamaterial sheet (plots of ϵ , μ , and σ shown in Fig. 3) with irregular geometry, submitted to an incident plane wave off-resonance (top) and in-resonance (bottom). The surface color, bar to the left, represents the out-of-plane electric field. To the right of each figure, a cross section of the film is showing the resistive losses in the material. They correctly predict high reflection and almost no losses when

the incident wave is off-resonance and lower reflection with appreciable loss at resonance. Figure 9(b) shows the reflection and transmission characteristics of the structure to show the on- and off-resonance responses, which were obtained from the scattering parameters. Another confirmation of behavior as expected is the fact that most of the losses occur close to the surface on the side of incident wave. Finally, the plots of the incident wave indicate that off resonance, reflected waves are interfering with the incident wave, whereas at resonance where the incident wave is absorbed, there is almost no interference.

V. CONCLUSION

We have used simulated and experimental scattering data from planar metamaterial absorber structures of unknown material properties and processed the data with a retrieval algorithm to obtain equivalent medium parameters for an analogous homogenized structure. The equivalent medium parameters permit rapid modeling of complex structures that are difficult and time consuming to simulate if their microscopic features are considered. The retrieval algorithm used verifies the approach from Ref. 8 to overcome branch ambiguity, inherent in the formulation, and verifies that this method works for structures on the margin of the homogenization criteria. The derived equivalent medium parameters

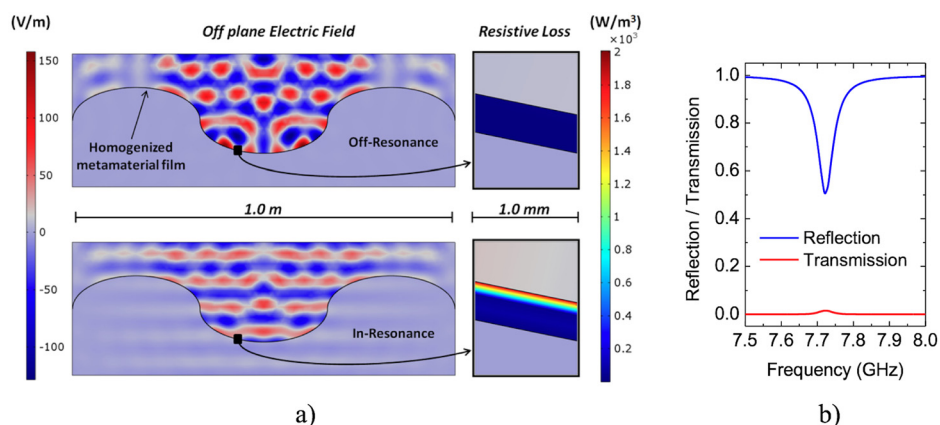


FIG. 9. (a) Propagation of a plane wave over a large area, oddly shaped metamaterial sheet. In this simulation, we used the homogenized equivalent parameters, retrieved from the metamaterial unit cell, whose characteristics are shown in Fig. 3. Surface colors indicate the off-plane electric field magnitude (left) and resistive loss on the metamaterial sheet (right). The right-hand side insets are magnifications of the region indicated by the black square (follow the arrow). (b) Reflection and transmission characteristics of the structure, obtained from the scattering parameters.

proved applicable to large-scale metamaterial structures and odd geometries. The method facilitates and accelerates scaling of metamaterials to simulate macroscale, complicated metamaterial geometries, all based on the data collected from a single representative prototype.

ACKNOWLEDGMENTS

This work was sponsored by the Office of Naval Research (ONR), under Grant (or Contract) No. N0001416WX01128. The authors would also like to thank Dr. Jesus Gil Gil and Dr. Brian Meyerhofer at the Naval Research Laboratory for performing the scattering parameter measurements.

¹T. Chen, S. Li, and H. Sun, *Sensors* **12**, 2742 (2012).

²B. Kearney, F. Alves, D. Grbovic, and G. Karunasiri, *Opt. Eng.* **52**, 013801 (2013).

³T. Hao, L. Hai-Tao, and C. Hai-Feng, *Chin. Phys. B* **23**, 025201 (2014).

⁴M. T. McMahan, M.S. thesis (Phys. Dept., Naval Postgraduate School, Monterey, CA, 2015).

⁵D. R. Smith, S. Schultz, P. Markos, and C. M. Soukoulis, *Phys. Rev. B* **65**, 195104 (2002).

⁶S. Arslanagic, T. V. Hansen, N. A. Mortensen, A. H. Gregersen, O. Sigmund, R. W. Ziolkowski, and O. Breinbjerg, *IEEE Antennas Propag. Mag.* **55**, 91 (2013).

⁷X. Chen, T. Grzegorzczak, B. Wu, J. Pacheco, Jr., and J. Kong, *Phys. Rev. B* **70**, 016608 (2004).

⁸S. Ramakrishna and T. Grzegorzczak, *Physics and Applications of Negative Refractive Index Materials* (CRC Press, Boca Raton, 2009), pp. 29–75.

⁹J. Hao, L. Zhou, and M. Qiu, *Phys. Rev. B* **83**, 165107 (2011).

¹⁰F. Alves, B. Kearney, D. Grbovic, N. V. Lavrik, and G. Karunasiri, *App. Phys. Lett.* **100**, 111104 (2012).

¹¹F. Alves, D. Grbovic, B. Kearney, N. V. Lavrik, and G. Karunasiri, *Opt. Express* **21**, 13256 (2013).

¹²L. La Spada, “Metasurface-epsilon near zero-based electromagnetic wave absorber,” in *Proceedings of the 9th International Conference on Body Area Networks*, London, UK, 29 September–1 October 2014, ICST (Institute for Computer Sciences, Social-Informatics and Telecommunications Engineering, Brussels, Belgium, 2014), pp. 310–315.